Geofluids (2008) **8**, 239–251 doi: 10.1111/j.1468-8123.2008.00223.x

Geological background of the Kairei and Edmond hydrothermal fields along the Central Indian Ridge: Implications of their vent fluids' distinct chemistry

H. KUMAGAI[1,2], K. NAKAMURA[1,3], T. TOKI[4], T. MORISHITA[5], K. OKINO[6], J.-I. ISHIBASHI[7], U. TSUNOGAI[8], S. KAWAGUCCI[4], T. GAMO[4], T. SHIBUYA[1], T. SAWAGUCHI[9], N. NEO[10], M. JOSHIMA[11], T. SATO[6] AND K. TAKAI[1,12]

[1]Precambrian Ecosystem Laboratory, Japan Agency for Marine-Earth Science and Technology (JAMSTEC), Natsushima-cho, Yokosuka, Kanagawa, Japan; [2]Institure for Research on Earth Evolution (IFREE), Japan Agency for Marine-Earth Science and Technology (JAMSTEC), Natsushima-cho, Yokosuka, Kanagawa, Japan; [3]Frontier Research Center for Energy and Resources (FRCER), School of Engineering, The University of Tokyo, Hongo, Bunkyo-ku, Tokyo, Japan; [4]Department of Chemical Oceanography, Ocean Research Institute (ORI), The University of Tokyo, Minamidai, Nakano-ku, Tokyo, Japan; [5]Frontier Science Organization, Kanazawa University, Kakuma, Kanazawa, Ishikawa, Japan; [6]Department Ocean Floor Geoscience, Ocean Research Institute (ORI), The University of Tokyo, Minamidai, Nakano-ku, Tokyo, Japan; [7]Department of Earth and Planetary Sciences, Faculty of Science, Kyushu University, Hakozaki, Higashi-ku, Fukuoka, Japan; [8]Earth and Planetary System Science, Faculty of Science, Hokkaido University, Kita-ku, Sapporo, Japan; [9]Department of Infomatics and Media Technology, Shohoku College, Atsugi, Kanagawa, Japan; [10]Graduate School of Science and Technology, Niigata University, Ikarashi, Niigata, Niigata, Japan; [11]Geological Survey of Japan, AIST, Higashi, Tsukuba, Ibaraki, Japan; [12]Subground Animalcule Retrieval (SUGAR) Project, Extremobiosphere Research Center (XBR), Japan Agency for Marine-Earth Science and Technology (JAMSTEC), Natsushima-cho, Yokosuka, Kanagawa, Japan

ABSTRACT

Hydrogen-rich hydrothermal areas, such as those in the Indian Ocean, may have had an influence on early evolution of life on Earth and thus have attracted interest because they may be a proxy for ancient ecosystems. The Kairei and Edmond hydrothermal fields in the Indian Ocean are separated by 160 km, but exhibit distinct fluid chemistry: Kairei fluids are hydrogen-rich; Edmond fluids are hydrogen-poor. At this region, the Central Indian Ridge shows an intermediate spreading rate, 48 mm year^{-1} as full rate, where the hydrothemal fields occur. Kairei field vent fluids show persistently high concentrations of H_2. The Kairei field seems to be unique among hydrogen-enriched hydrothermal regions: most similar hydrogen-rich hydrothermal activity occurs along slowly spreading ridge, <40 mm year^{-1}. The geological and tectonic aspects of the Kairei and Edmond hydrothermal fields were studied to try to elucidate geological constraints on hydrogen production. Visual observations of the seafloor near Kairei from a submersible revealed olivine-rich plutonic rocks with olivine gabbro-troctolite-dunite assemblages exposed within 15 km of the vent field, with serpentinized ultramafic mantle rocks on the Oceanic Core Complex (OCC). The OCC area might be a recharge zone of Kairei hydrothermal activity producing H_2-rich vent fluids. The chaotic seafloor within 30 km of the Kairei field reflects a magma-starved condition persisting there for 1 Myr. Asymmetric geomagnetic and gravity anomalies near the Kairei field can be used to infer that patchy olivine-rich intrusions are scattered within mantle ultramafics, where infiltrated seawater reacts with magma and ultramafic rocks or olivine-rich rocks. The heterogeneous uppermost lithosphere containing shallow olivine-rich rock facies surrounding the Kairei field provides abundant H_2 into the vent fluid through serpentinization. The hydrogen-rich Kairei field is hosted by basalt, with mafic-ultramafic olivine-rich lithology; the ordinary, hydrogen-poor Edmond field is hosted by a normal basaltic lithology. The contrasting geochemical signatures of the two fields reported here can also be found in ancient rocks from a juvenile Earth. This suggests that lithology-controlled generation of hydrogen may have operated for a long time and be relevant to the origin of life on Earth.

Key words: hydrogen production, Kairei hydrothermal field, oceanic core complex, serpentinization, troctolite, Uraniwa Hills

Received 10 May 2008; accepted 24 September 2008

Corresponding author: Hidenori Kumagai, Research Scientist, Research Program for Mantle-Core Dynamics, Institute for Research on Earth Evolution (IFREE), JAMSTEC (Japan Agency for Marine-Earth Science and Technology), 2-15 Natushima-cho, Yokosuka, Kanagawa 237-0061, Japan.
Email: Kumagai@jamstec.go.jp. Tel: +81-46-867-9333. Fax: +81-46-867-9315.

Geofluids (2008) **8**, 239–251

INTRODUCTION

Seafloor hydrothermal fields have attracted great interest in many disciplines of Earth and biological sciences since their initial discovery in the late 1970s (Hessler & Kaharl 1995). A remarkable feature of the habitat around hydrothermal fields is that lithotrophic micro-organisms are independent of energy derived from sunlight (cf. Takai *et al.* 2006). Such an environment resembles early stages of the Earth's history: pre-photosynthetic worlds founded in the dark abyss. Consequently, some predominant ideas about the origin of life specifically relate to deep-sea hydrothermal systems.

Such postulated models of early Earth history have come to constitute part of an important field of science. Microbiologists have proposed various possibilities for establishment of microbial ecosystems in the very early stages of Earth history. Among the proposed scenarios, a modern proxy ecosystem for the earliest stages in our evolution favours hydrogen-rich fluids in abyssal hydrothermal systems (Takai *et al.* 2004). Therefore, understanding the mechanism that supplies hydrogen to the vent fluids will presumably help understand the earliest stages of evolution of life on Earth. This is one reason why such hydrothermal fields enriched in hydrogen have been investigated extensively in the last decade.

To date, most hydrogen-rich hydrothermal activity has been found along the slowly spreading, approximately 40 mm $year^{-1}$ or less, Mid Atlantic Ridge (MAR). Among them, the activities of the Rainbow, Lost City, and Logachev hydrothermal fields have been well documented (Charlou *et al.* 2002; Kelley *et al.* 2005). Recently, two more examples have been explored (Beltenev *et al.* 2007; Walter *et al.* 2008). With limited supply of magma near the slowly spreading ridges, deep lithologies of oceanic lithosphere, plutonic gabbros or mantle peridotites, become widely exposed on the seafloor. Frequently, such exposures form dome-shaped geologic bodies that designated Oceanic Core Complexes (OCCs). In fact, the Lost City field is located on one of the OCCs: the Atlantis Massif (Kelley *et al.* 2005). Among abiotic sources of hydrogen, serpentinization of mantle peridotites is favoured near OCCs because of the greater and more sustained production of hydrogen than that by other mechanisms, e.g. radiolysis, dyke-penetration into shallow crust, or silicate catalysis at fault areas (e.g. Bach 2007; Blair *et al.* 2007).

The Indian Ocean hydrothermal fields occupy a unique position to facilitate our understanding of the hydrogen production in the Mid-Oceanic Ridge (MOR) environment. Two active hydrothermal fields, Kairei and Edmond, exist along the Central Indian Ridge (CIR) showing an intermediate spreading rate (~48 mm $year^{-1}$). These two hydrothermal fields show geochemically-distinct signatures in their vent fluids, despite being only 160 km apart. The Kairei field seems to be a unique case of hydrogen-rich hydrothermal activity outside of the slowly spreading ridge environment; it is located at 25.32°S, 70.04°E towards the northern end of the first segment of CIR (CIR-1), counted from the Rodriguez Triple Junction (25.5°S, 70°E; Fig. 1), which incidentally was the first hydrothermal field discovered in the Indian Ocean (Gamo *et al.* 2001). In contrast, the neighbouring Edmond field shows normal or lower hydrogen concentrations typical of a MOR environment (Gallant & Von Damm 2006). It is located at 23.88°S, 69.60°E, near the northern end of the third segment of the CIR, CIR-3 (Van Dover *et al.* 2001). A model was previously proposed to explain the unique characteristics of Kairei vent fluids in comparison to the Edmond fluids (Gallant & Von Damm 2006): sub seafloor precipitation of sulphide, generating H_2 as a by-product. This model excludes the possibility that alteration of ultramafic, olivine-rich mantle rocks provides abundant hydrogen to vent fluid, because they did not find such rocks in the vicinity. However, no exploration of the wider regional geological environment has been reported prior to our study.

In this paper, we report a comprehensive investigation of the linkage between the fluid chemistry and the tectono-geological environment of both the Kairei and Edmond hydrothermal fields. For this purpose, local geological observations coupled with regional geophysical surveys of the areas surrounding each hydrothermal field were performed using a manned JAMSTEC submersible (Shinkai6500) in January 2006 during the YK05-16 cruise.

MATERIALS AND METHODS

Fluid chemistry revisited

Hydrothermal fluids were sampled using gas-tight bottles (WHATS sampler; Tsunogai *et al.* 2003; Saegusa *et al.* 2006), which were attached to the Shinkai6500 manned

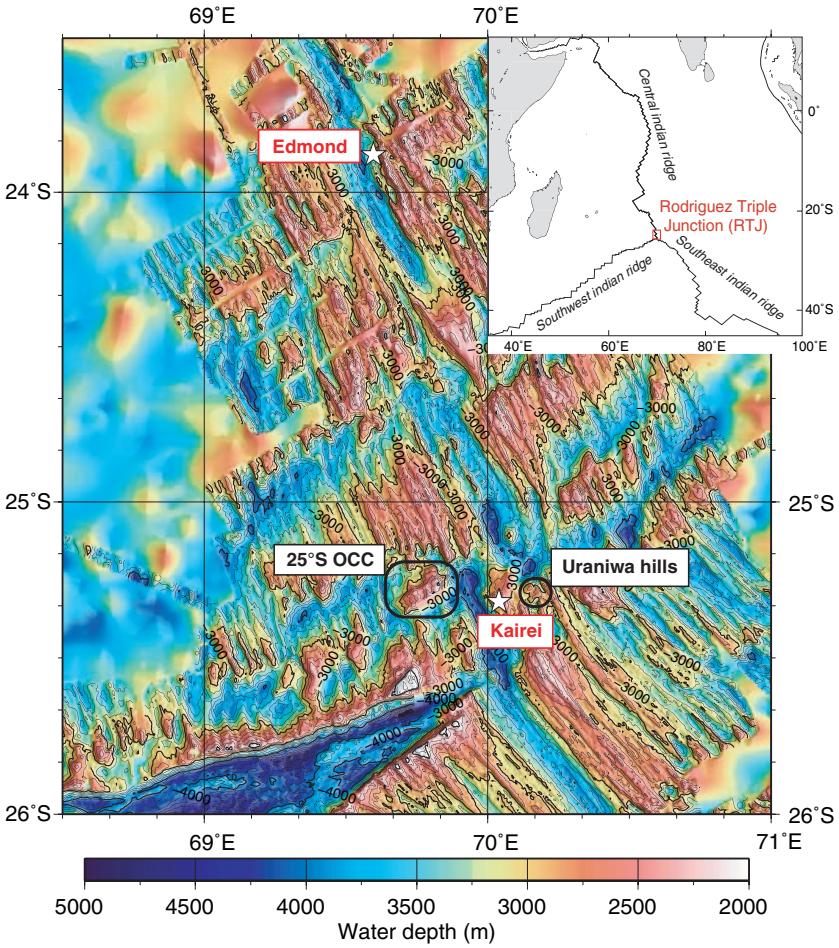

Fig. 1. Generalized bathymetry of the studied area. Data sources of multi narrow beam bathymetry: KH93-3, KR00-05, YK01-15, YK05-16 [http://www.jamstec.go.jp/dsr/] and the cruises using French vessels (Briais 1995).

submersible. Immediately after the dive was completed, sampled fluids for gas and water chemistry were processed onboard. All dissolved gases were separated from the fluid solution using a gas extractor (Konno *et al.* 2006). The extracted gases were stored in 50-ml metallic flasks and analysed onshore after the cruise. The residual fluids in the gas extractor were transferred to polyethylene flasks after filtration and were analysed for water chemistry. At Hokkaido University, the carbon isotopic compositions of ΣCO_2 and CH_4 with their contents were assessed using isotope-ratio-monitoring GC/MS. At the Ocean Research Institute of the University of Tokyo (ORI), H_2 gas concentrations and isotope compositions of hydrogen were determined using a continuous flow isotope ratio mass spectrometer system (Kawagucci *et al.* 2007): the isotopic compositions will be reported elsewhere (Kawagucci *et al.*, in preparation). Elemental composition of the water samples were determined at Kyushu University. The concentrations chloride, potassium and sulfate were determined by Mohr method, by flame spectrophotometry and by ion chromatography, respectively. Other major (Na, Ca, Mg, Si) and minor (Mn, Sr, Ba, Fe) elements were measured using ICP-AES after appropriate dilution of the samples. Alkalinity was determined by titration with hydrochloric acid with Gran plot estimation of the end-point on board (Table 1). pH and H_2S were also measured on board.

Seafloor observation, bathymetry, and geophysics

During the YK05-16 research cruise, visual geological and volcanological observations from a manned submersible were guided using detailed bathymetric information obtained using a multi-narrow beam echo sounder (MNBES, SeaBEAM 2112) of the R/V Yokosuka. Such multi-beam bathymetry is the minimum requirement for geological study of the seafloor. It enables samples to be taken as precisely as those taken on land. In addition, a region-wide bathymetric survey with gravity and geomagnetic observations was conducted during the expedition. Linkages between the respective water chemistries of two hydrothermal fields and geological environments or microbial communities were also targeted. Through visual observation, lava fragments partially embedded in the sediments

were sampled using the Shinkai6500 submersible's manipulators.

Rock chemistry

The rock samples used for this study were obtained using the submersible's manipulators under visual observation through the submersible's viewport with video recording of their occurrence. Fresh glass shards of lava fragments were selected for analyses from among a suite of rock samples obtained during the submersible dives in the cruise.

Major element compositions of hand-picked, glassy, lava fragments (SiO_2, TiO_2, Al_2O_3, FeO, MnO, MgO, CaO, Na_2O, K_2O, and P_2O_5; Table 2A) were assessed at Kanazawa University using an electron microprobe (JXA-8800; JEOL). The analyses were performed using an accelerating voltage of 15 kV and a beam current of 10 nA using a 10-μm-diameter-beam. The X-ray peaks were counted for 10 s and backgrounds in both high-wavelength and low-wavelength sides were measured for 5 s. In addition, JEOL software using ZAF corrections was used. No loss of Na was observed during the analysis under analytical conditions.

Trace-element compositions of lava glasses (Table 2B) were determined using an ICP-MS (7500S; Agilent Technologies Inc.) equipped with an ArF excimer laser ablation system (193 nm, 5 Hz, GeoLas Q-plus; MicroLas Lasersystem GmbH) at Kanazawa University (Ishida *et al.* 2004). Ablation of a 50-μm-diameter area was necessary to avoid microcrystal ablation. The peak of ^{43}Ca was monitored as an internal standard, as described in Longerich *et al.* (1996); the NIST SRM 612 glass was used as the calibration standard. A glass standard was analysed initially before each batch of analyses (each batch being eight analyses) with a linear drift correction of standard intensities applied between each calibration. The elemental concentrations of glasses were taken from Pearce *et al.* (1997). Detailed analytical procedures and the precision and accuracy of the data on NIST SRM 614 and BCR-2G reference standard glasses with identical analytical conditions appear in Morishita *et al.* (2005a,b).

RESULTS

Fluid chemistry

Plots of selected major elements and H_2 concentrations versus Mg concentration in sampled fluids display linear relationships representing mixing between a single or a few hydrothermal end-member and ambient seawater in each hydrothermal field (Fig. 2 A–F). Estimated compositions of end-member fluids for each vent area are listed in Table 1. A remarkable feature of the Kairei hydrothermal fluid includes its much greater H_2 concentration in the end-member than in seawater: 2.5–3.7 mmol kg^{-1} of H_2 versus 1 nmol kg^{-1} in seawater (Table 1; Fig. 2F; McLaughlin-West *et al.* 1999). This elevated H_2 concentration range lies within the reported variation in the field: 2.5–8.5 mmol kg^{-1} (Van Dover *et al.* 2001; Takai *et al.* 2004; Gallant & Von Damm 2006). On the other hand, the H_2 concentrations in the Edmond fluids are markedly low: 0.055–0.111 mmol kg^{-1}. This concentration range resembles that found elsewhere on the East Pacific Rise and Mid Atlantic Ridge hosted by mid-ocean ridge basalts (MORB).

Another stark difference between the fluid chemistries of the areas is that of the Na concentration and Na/Cl ratio. In Kairei, the Na/Cl ratio of the fluid end-member corresponds well to that of seawater, approximately 0.85 (Nozaki 2001), which is consistent with the phase separation of the infiltrated seawater beneath the seafloor. Slightly concentrated Na from the seawater of 480–520 mmol kg^{-1} suggests that their origin is the brine part of the separated phases. Here, the Na concentration in seawater was 465 mmol kg^{-1}. On the other hand, Na/Cl ratios of vent fluids in the Edmond field are much lower, <0.75, although their Na concentrations are much higher, 700–710 mmol kg^{-1}, than those of seawater. This relates to the much more strongly enriched Cl concentration of the fluid end-member in the Edmond field, 930–970 mmol kg^{-1} than the 542 mmol kg^{-1} in seawater. Similar to Na, other alkaline and alkaline earth elements, e.g. K and Ba, are strongly enriched in Edmond fluids as a factor of two or more compared to those in Kairei fluids. Respective K concentrations in Kairei and Edmond are 12.5–13.8 mmol kg^{-1} and 39–42 mmol kg^{-1}; Ba concentrations in fluid are upto 43 μmol kg^{-1} for Kairei and upto 120 μmol kg^{-1} for Edmond.

Visual sea floor observation and regional bathymetry in a segment scale

Local geological conditions near Kairei and Edmond are broadly similar, with respect to their volcanic features, for about the 1–2 km distance over which the areas were explored using the submersible (Fig. 3). However, the immediate vicinities of the vent areas were covered with hydrothermal precipitates and collapsed dead chimneys. The Kairei hydrothermal field developed on the shoulder of the west-facing slope of a recently formed abyssal hill of CIR-1, designated as Hakuho Knoll. It comprises piles of flat or lobate sheet flows (Fig. 3A). Similarly, the Edmond field developed on another abyssal hill of CIR-3. The vicinity of the Edmond field is a flat surface with partly wrinkled lava flows, largely covered by a layer of sediment <30 cm in thickness, as measured using a carry-on sub bottom sound profiler (Strata Box; SyQwest Inc., Warwick, RI, USA). In addition to hydrothermal precipitates, the

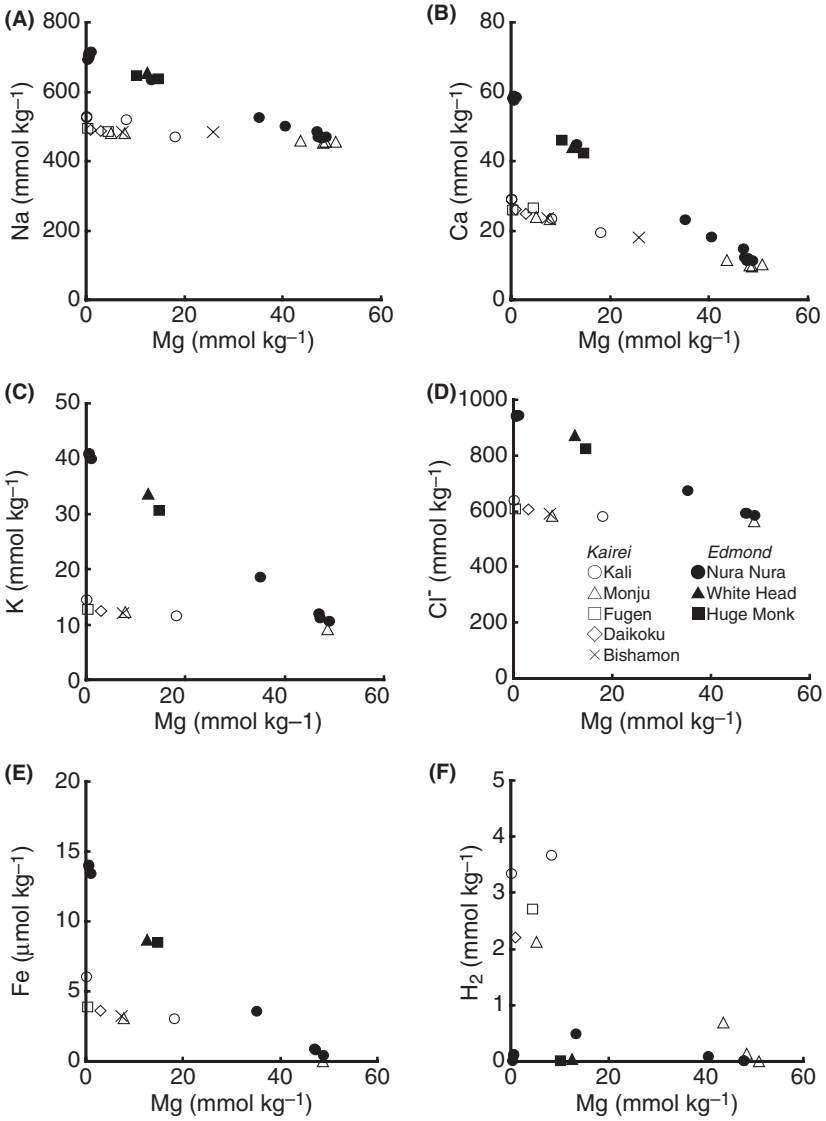

Fig. 2. Relationships of selected major elements and H_2 concentrations versus Mg concentration in sampled fluids. Symbols are shown in sub-panel (D).

seafloor comprises basaltic pillows and massive flows (Fig. 3B). The flow surface partly showed a flat, lobate sheet shape or a smooth or slightly wrinkled surface, indicating a higher flow rate than those observed as pillow piles.

In terms of tectonics at the segment-scale of CIR, the environments of Kairei and Edmond differ greatly. The morphological contrast between the vicinities of the two hydrothermal fields might influence on the geological pathway of the recharged vent fluid.

Near the Kairei field, the regional seafloor morphology is distinctly heterogeneous within 30 km from the current ridge axis, roughly reflecting the most recent 1 Myr of local seafloor spreading. Abyssal hills, which normally develop parallel to the present day ridge axis, are widely disorganized away from CIR-1 (Fig. 4A). For example, a deep linear shape is visible at 70°12′E, 25°16′S (Fig. 4A) associated with partly symmetric abyssal hills on both sides, which might be an abandoned ridge axis. This might, in turn, have originated from the unstable nature of seafloor spreading in the area accompanied with a ridge jump.

In contrast, in the area off CIR-3 around the Edmond field, regular ridge-parallel abyssal hills extending to ca. 60 km away from the ridge axis were not disorganized (Fig. 4B). Almost at the western edge of the survey area off CIR-3, a corrugated seafloor was mapped with a partly ridge-perpendicular alignment. Apparently, CIR-3 has maintained its robust magmatism for approximately 2 Myr.

CIR-1 is also characterized by two well-defined Oceanic Core Complex (OCC) structures found within 20 km of the Kairei field. One is located 20 km west of the Kairei field, currently across the ridge axis (25°S OCC; Mitchell *et al.* 1998). The other is located 15 km east of the Kairei field, hereinafter designated as Uraniwa Hills, that was

Table 1 Estimated end member compositions of hydrothermal fluids sampled from Kairei and Edmond fields. –: not analysed.

Area	Vent name	Depth (m)	Na mmol kg^{-1}	Ca mmol kg^{-1}	K mmol kg^{-1}	Si mmol kg^{-1}	Cl^- mmol kg^{-1}	SO_4^{2-} mmol kg^{-1}
Kairei Field	Kali	2450	518 ± 15	27.2 ± 0.8	13.8 ± 0.6	16.0 ± 0.7	623 ± 6	−0.17 ± 0.02
	Monju	2420	484 ± 20	25.6 ± 1.0	12.8 ± 0.8	16.7 ± 0.9	589 ± 7	0.93 ± 0.48
	Fugen	2420	489 ± 19	26.7 ± 1.0	12.7 ± 0.7	16.8 ± 0.9	606 ± 7	−0.06 ± 0.02
	Daikoku	2443	489 ± 18	25.9 ± 1.0	12.7 ± 0.7	16.8 ± 0.9	611 ± 7	6.93 ± 0.45
	Bishamon	2432	490 ± 26	25.9 ± 1.2	12.5 ± 0.8	16.9 ± 0.9	595 ± 7	−0.63 ± 0.39
Edmond Field	Nura Nura	3280	704 ± 14	58.5 ± 1.2	40.8 ± 1.2	20.2 ± 0.6	946 ± 6	−0.30 ± 0.02
	White Head	3290	713 ± 32	54.9 ± 2.3	41.5 ± 2.4	19.6 ± 1.1	973 ± 15	−8.30 ± 0.80
	Huge Monk	3290	697 ± 32	55.3 ± 2.3	39.1 ± 2.3	18.2 ± 1.1	928 ± 15	−2.19 ± 0.99

Area	Vent name	Depth (m)	pH	Alkalinity mmol kg^{-1}	Mn μmol kg^{-1}	Sr μmol kg^{-1}	Ba μmol kg^{-1}	Fe μmol kg^{-1}
Kairei Field	Kali	2450	3.4	−0.456 ± 0.006	828 ± 35	74.2 ± 3.3	42.5 ± 2.3	5.40 ± 0.25
	Monju	2420	3.6	−1.24 ± 0.04	848 ± 44	66.5 ± 4.2	10.6 ± 0.6	3.67 ± 0.19
	Fugen	2420	3.4	−0.288 ± 0.004	840 ± 43	68.2 ± 3.5	14.8 ± 0.8	3.86 ± 0.20
	Daikoku	2443	3.4	−0.788 ± 0.015	828 ± 42	66.7 ± 3.7	9.54 ± 0.48	3.86 ± 0.20
	Bishamon	2432	3.4	−1.09 ± 0.04	828 ± 48	66.6 ± 0.3	5.51 ± 0.29	3.73 ± 0.20
Edmond Field	Nura Nura	3280	3.3	−0.397 ± 0.006	1360 ± 40	181 ± 6	102 ± 3	13.9 ± 0.4
	White Head	3290	3.1	−1.34 ± 0.08	1420 ± 80	175 ± 11	49.7 ± 2.7	11.5 ± 0.7
	Huge Monk	3290	3.2	−1.55 ± 0.10	1360 ± 80	177 ± 11	119 ± 7	11.8 ± 0.7

Area	Vent name	Depth (m)	H_2S mmol kg^{-1}	$\sum CO_2$ mmol kg^{-1}	H_2 mmol kg^{-1}	CH_4 μmol kg^{-1}	$\delta^{13}C_{co2}$ ‰ PDB	$\delta^{13}C_{CH4}$ ‰PDB
Kairei Field	Kali	2450	4.81 ± 0.17	9.47 ± 0.47	3.71 ± 0.14	123 ± 6	−5.3 ± 0.3	−9.8 ± 0.3
	Monju	2420	–	8.57 ± 0.58	2.48 ± 0.12	163 ± 11	−5.1 ± 0.3	−17.6 ± 0.3
	Fugen	2420	6.40 ± 0.07	10.1 ± 0.7	2.97 ± 0.15	202 ± 14	−5.1 ± 0.3	−18.0 ± 0.3
	Daikoku	2443	5.90 ± 0.07	–	–	–	–	–
	Bishamon	2432	6.06 ± 0.09	–	–	–	–	–
Edmond Field	Nura Nura	3280	3.98 ± 0.03	13.7 ± 0.5	0.1116 ± 0.0037	314 ± 12	−5.4 ± 0.3	−13.5 ± 0.3
	White Head	3290	1.83 ± 0.04	9.95 ± 0.71	0.0556 ± 0.0031	283 ± 20	−5.0 ± 0.3	−12.5 ± 0.3
	Huge Monk	3290	1.15 ± 0.03	15.8 ± 1.1	–	233 ± 16	−5.8 ± 0.3	−13.0 ± 0.3

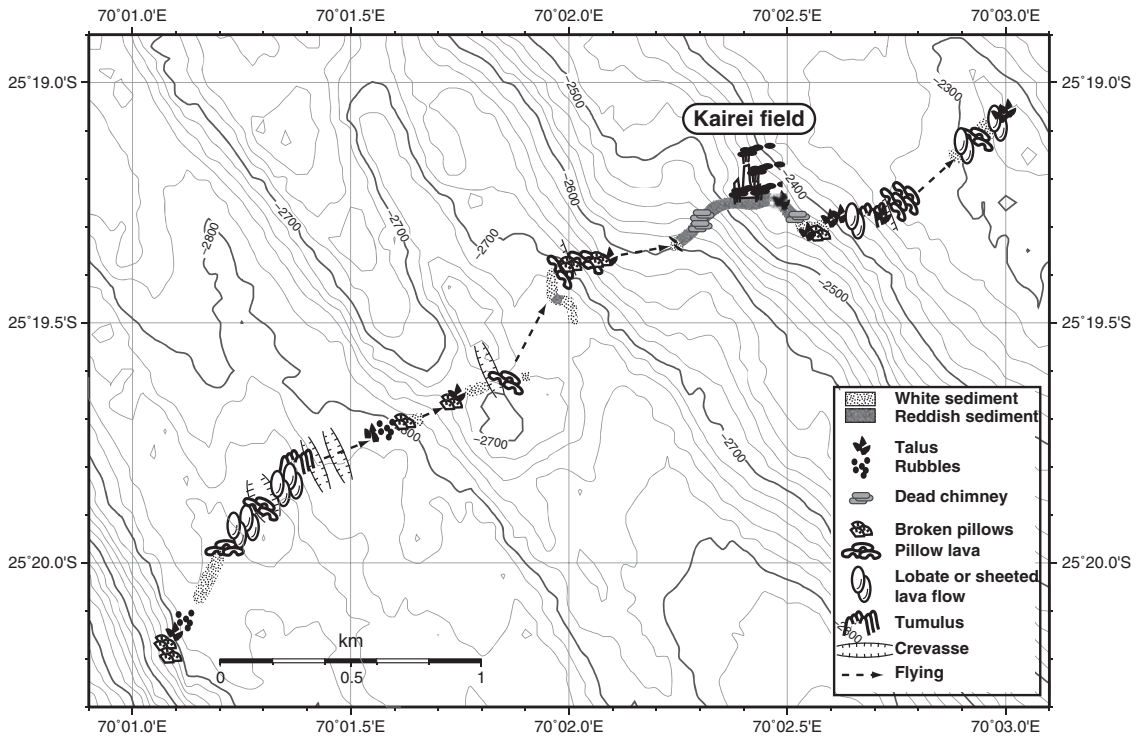

Fig. 3. Route maps of submersible dives. Data source of multi narrow beam bathymetry: YK05-16 [http://www.jamstec.go.jp/dsr/]. (A) Route map of the Shinkai6500 submersible dive #918 (dive observer: H. Kumagai). (B) Route map of the Shinkai6500 submersible dive #923 (dive observer: T. Shibuya).

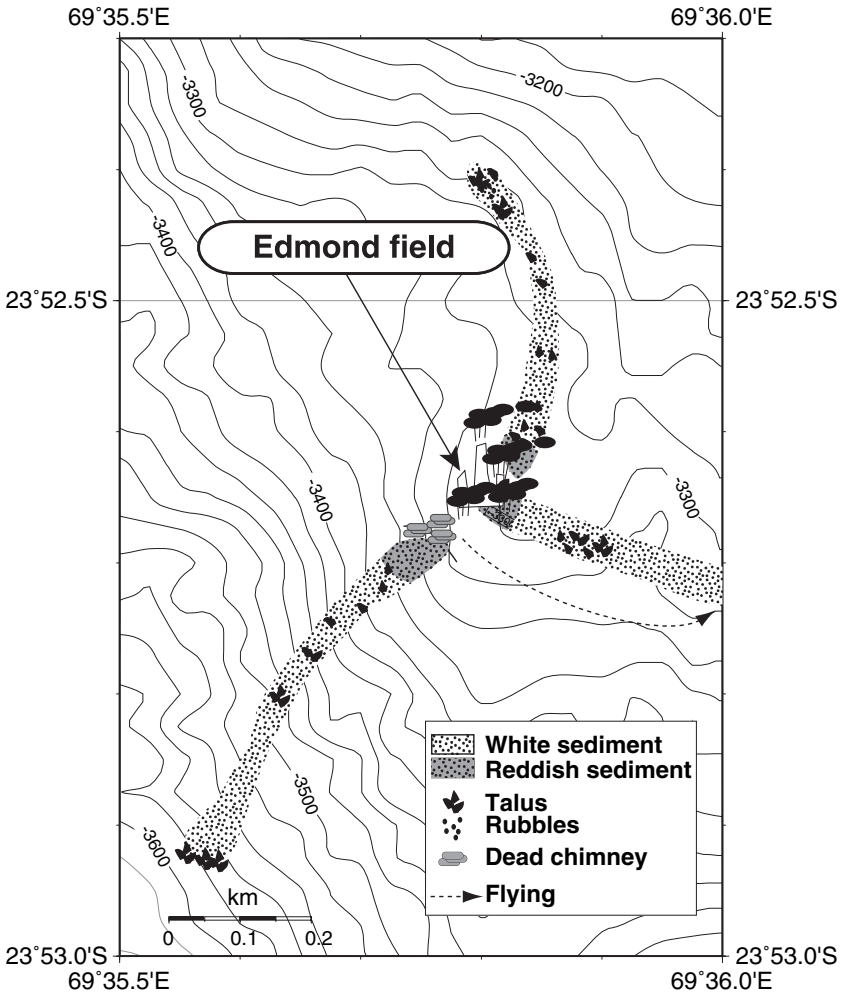

Fig. 3B. Continued

newly recognized in our expedition. Such OCCs are mainly found under magma-starved conditions near slowly-spreading ridges, although the Central Indian Ridge (CIR) has been classified as having an intermediate rate of seafloor spreading. Actually, two weathered peridotites, of which possible protoliths are lherzolite and harzburgite, were sampled among the basalt- to gabbro-dominated rock suites on the 25°S OCC (Fig 4A). At Uraniwa Hills, olivine-abundant mafic plutonic rocks including troctolites and olivine gabbros were also sampled in addition to a dunite (Fig.4A; Morishita *et al.*, in preparation; Nakamura and Bach, submitted to EPSL). In addition, Hellebrand *et al.* (2002) reported that an ultramafic rock had also been obtained on the top of an obliquely elongated hill, 30° oblique in an anti-clockwise direction from the current ridge axis. Consequently, a substantial fraction of shallow crust near the Kairei field, where basaltic volcanic rocks were previously anticipated, actually consists of ultramafic mantle material and olivine-rich plutonic rocks.

Rock chemistry

All lava samples near the two hydrothermal fields are basaltic. Most of the compatible element contents of the lava samples near hydrothermal fields both overlap with a rather primitive nature: the Kairei field lava has 50.6–51.5 wt% SiO_2, 8.4–8.9 wt% MgO and 7.9–8.6 wt% FeO, whereas the lava of the Edmond field contains 50.8–51.2 wt% SiO_2, 7.6–8.0 wt% MgO, and 8.2–8.6 wt% FeO. Because of this similarity, the differences of Mg#, defined as $Mg^{2+}/(Mg^{2+}+ Fe^{2+})$ in molar proportions, in both areas are of a similar range: 0.66–0.64 for Kairei and 0.63–0.62 for Edmond, respectively.

In contrast, such similarity is not the case for incompatible elements. The concentrations of incompatible elements are high in the Edmond lava but low in the Kairei lava. This is readily apparent from their K_2O, Na_2O and TiO_2 concentrations. Kairei lava has <0.06 wt% of K_2O, 2.65–3.10 wt% of Na_2O and 1.04–1.24 wt% of TiO_2; Edmond lava has 0.11–0.15 wt% of K_2O, 3.08–3.22 wt% of Na_2O

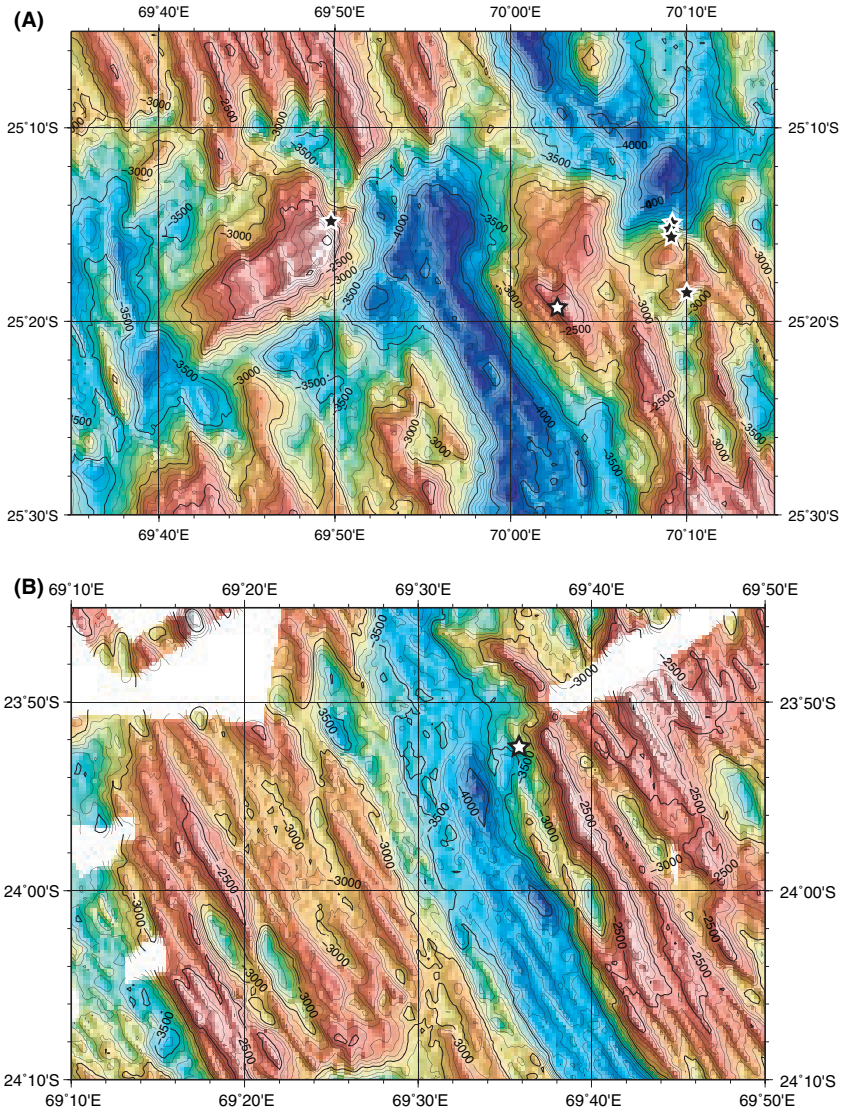

Fig. 4. Regional bathymetry around each hydrothermal field indicating as an open star. The closed stars in panel A (Kairei field) indicated the locality where either serpentinized peridotites or troctolites were sampled. Data source of multi narrow beam bathymetry: YK05-16 [http://www.jamstec.go.jp/dsr/]. (A) Kairei. (B) Edmond.

and 1.26 –1.42 wt% of TiO_2. All lava samples fall in the area of tholeiite in an alkaline diagram (Macdonald & Katsura 1964).

Such a depleted nature of Kairei lava can be clarified by observation of its trace elements. Although all lava samples from both areas show as depleted a nature in trace elements as do other MORB, the lava samples near the Kairei field are greatly depleted compared to those of the Edmond field. The La/Sm normalized to CI chondrite, expressed as (La/Sm)*n*, of both Kairei and Edmond areas are 0.41–0.5 and 0.72–0.80 respectively. Another normalization can be applied to emphasize this contrast. The Edmond lavas are less depleted in trace elements than 'Normal MORB' (Sun & McDonough 1989), of which (La/Sm)*n* is 0.61. In contrast, the Kairei lavas are more depleted than those in the normal MORB. Therefore, in a trace element diagram, where the elements are ordered by their incompatibility, the Edmond lava is expressed by curves elevated from the horizontal line on the left, highly incompatible trace element side, but Kairei lavas form valleys on that side (Fig. 5). Interestingly, the Th/Nb values of Kairei lava vary widely, 0.046–0.109, contrasted with the narrow range of Edmond lava: 0.070–0.085. This Th/Nb range results from the variable concentrations of Nb in Kairei lavas: 0.4–0.9 ppm.

DISCUSSION

Geological framework of the two distinct hydrothermal fields

Recent observations have revealed a laterally heterogeneous lithosphere at shallow depths surrounding the Kairei vent area with some exposure of plutonic and ultramafic mantle rock on the seafloor. Typical abyssal peridotites were sampled at the 25°S OCC in the western side of the Kairei hydrothermal field. In addition, a suite of olivine-rich mafic plutonic rocks (13 troctolites and 5 olivine gabbros) and a dunite were sampled from Uraniwa Hills. Those rocks might be members of the MOHO transition zone in usual layered uppermost lithosphere, which originated from the melt-rock reaction or as cumulates from mafic magma precipitating into the bottom of the magma chamber (Nakamura and Bach, submitted to EPSL).

Considering the possible heterogeneous structure in the shallow lithosphere in the H_2-rich area of CIR-1, the unique geochemical nature of the vent fluid of Kairei hydrothermal field is attributable to the lithological uniqueness of the pathway of recharged seawater. The occurrences of the troctolites or a dunite on the seafloor, which are normally anticipated near the bottom of the magma chamber as cumulate rocks, indicate a heterogeneous structure of the shallow lithosphere generated under magma-starved circumstances. Under such conditions, deficiencies of magma supply compared to the requirement for seafloor spreading are typically compensated by extension and exposure of a deeper part of the lithosphere. The disturbed alignment of abyssal hills indicates that a non-steady state of volcanic seafloor spreading has persisted for 1–2 Myr. This is further supported by the asymmetric position of the Brunhes-Matsuyama boundary on both sides of CIR-1, which implies the possibility of a ridge jump or asymmetric spreading that generates the OCC. Such an asymmetry was also reported for both the Bouguer anomaly and magnetization at the CIR-1 (Honsho *et al.* 1996). The calculated Residual Mantle Bouguer Anomaly of gravity in the CIR-1 also shows that denser materials than those anticipated by the standard cooling model are located in the eastern CIR-1 (Wakabayashi 2003). Judging from the bathymetry obtained during the expedition, up to several tens of kilometers from the Edmond field, normal well-layered mafic crust underlies most of the seafloor.

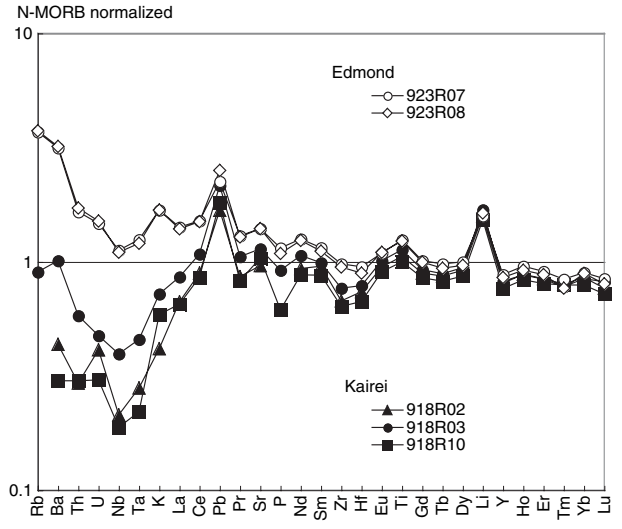

Fig. 5. Trace element diagram of glass shards of lava samples. The values plotted were normalized by the composition estimated as 'Normal MORB' (Sun & McDonough 1989).

Relation between fluid and rock chemistries

Among the major elements dissolved in vent fluids, highly incompatible alkaline and alkaline earth elements (K, Rb, and Ba) seem to reflect the geochemical character of surrounding lava because these elements have no major sink during hydrothermal reaction. It has been pointed out that these elements are simply depleted in hydrothermally altered MORB, reflecting leaching of these elements from rocks to hydrothermal fluid (e.g., Nakamura *et al.* 2007). In both hydrothermal fields, most basalts show a rather primitive character with approximately 8wt% of MgO and have almost identical major element compositions (Table 2A). However, the lava around Kairei field is depleted in K, Rb, and Ba by factors of three, ten, and five respectively (Table 2A). Indeed, concentrations of K and Ba in Edmond fluids are three and five times higher, respectively, than those in the Kairei fluids. No data are available for Rb in the Kairei and Edmond fluids.

In contrast to the highly incompatible elements described above, concentrations of Na and Ca in hydrothermal fluids are considered to be controlled by phase equilibria for primary and secondary minerals in reacted MORB (e.g. Berndt *et al.* 1989; Berndt & Seyfried 1993). Although the Na/Cl ratio of Kairei fluid is almost identical to that of ambient seawater, Edmond fluids exhibit a noticeably lower Na/Cl ratio. This depletion of Na/Cl in Edmond fluid is accompanied by an increase of Ca/Cl. As a consequence, Gallant & Von Damm (2006) suggested that albitization of Edmond host rock had occurred explaining the composition of Na and Ca in the hydrothermal fluids. Although Na concentration of hydrothermal fluids is mostly controlled by albitization, the Ca concentration of hydrothermal fluid depends not only on albitization but also on decomposition of clinopyroxene (Nakamura *et al.* 2007). This could plausibly account for the noticeably higher Ca/Cl ratios of Kairei fluids than seawater, despite their seawater-equivalent Na/Cl ratios. Nonetheless, based on the Na/Cl ratios, hydrothermal fluids from Edmond appear to represent ongoing albitization

Table 2 (A) Major element composition and trace element concentration for lava samples from vent vicinity.

	Kairei						Edmond				Standard	
wt%	918R02	*n* = 19	918R03	*n* = 13	918R10	*n* = 12	923R07	*n* = 18	923R08	*n* = 11	BCR-2G	*n* = 16
SiO_2	50.9	0.3	51.5	0.2	50.9	0.2	51.1	0.2	51.0	0.3	54.6	0.4
TiO_2	1.11	0.07	1.19	0.06	1.06	0.05	1.37	0.07	1.30	0.08	2.33	0.07
Al_2O_3	16.3	0.2	16.0	0.1	16.1	0.1	15.8	0.2	15.8	0.1	13.6	0.2
FeO	8.2	0.2	8.4	0.3	8.1	0.2	8.5	0.2	8.6	0.3	12.5	0.3
MnO	0.16	0.04	0.17	0.04	0.15	0.03	0.15	0.04	0.16	0.03	0.19	0.05
MgO	8.7	0.2	8.4	0.1	8.7	0.1	7.8	0.1	8.0	0.1	3.7	0.1
CaO	11.8	0.2	11.5	0.2	11.9	0.1	11.2	0.2	11.1	0.1	7.2	0.2
Na_2O	2.7	0.1	3.0	0.1	2.8	0.1	3.2	0.1	3.1	0.1	3.3	0.1
K_2O	0.03	0.02	0.05	0.02	0.04	0.02	0.12	0.02	0.12	0.03	1.73	0.08
P_2O_5	< 0.1		0.11	0.07	0.07	0.06	0.13	0.06	0.13	0.05	0.39	0.08
Total	99.8	0.5	100.4	0.5	99.9	0.3	99.3	0.5	99.2	0.5	99.5	0.7

	Kairei						Edmond				Standard	
ppm	918R02	*n* = 5	918R03	*n* = 4	918R10	*n* = 4	923R07	*n* = 5	923R08	*n* = 3	BCR-2G	*n* = 9
Li	6.8	0.2	7.3	0.1	6.6	0.2	6.8	0.2	7.0	0.1	11.5	0.3
B	2.2	0.4	2.5	0.4	1.9	0.5	2.4	0.2	2.2	0.7	7.0	0.6
Sc	33	0.5	34	0.4	34	0.5	35	0.4	35	0.4	32.1	0.7
V	260	5	266	6	252	6	266	6	269	5	485	9.7
Cr	425	6	413	7	435	6	367	9	376	10	19	1
Co	48	1.0	48	0.5	48	0.8	43	1.1	45	0.9	44	1.0
Ni	142	4	133	2	131	5	112	3	125	2	21	2
Rb	< 0.2		0.51	0.10	< 0.2		2.07	0.09	2.09	0.05	59	1.3
Sr	86.6	1.0	102.4	1.0	93.5	1.2	125.6	0.8	125.7	0.5	319	3
Y	22.5	0.2	23.0	0.4	21.4	0.2	24.6	0.2	23.9	0.3	28.6	0.4
Zr	49.8	0.4	56.7	0.8	47.1	0.8	72.5	0.6	70.2	0.6	146	2
Nb	0.50	0.03	0.92	0.03	0.44	0.03	2.62	0.06	2.56	0.08	12.4	0.2
Cs	< 0.1		< 0.1		< 0.1		< 0.1		< 0.1		1.4	0.0
Ba	2.74	0.08	6.37	0.30	1.90	0.02	19.9	0.4	20.1	0.4	660	7
La	1.67	0.05	2.15	0.02	1.63	0.06	3.55	0.05	3.48	0.06	23.0	0.4
Ce	6.68	0.07	8.09	0.08	6.42	0.14	11.33	0.06	11.23	0.16	53.8	0.9
Pr	1.14	0.05	1.39	0.02	1.09	0.01	1.71	0.04	1.69	0.03	6.27	0.14
Nd	6.82	0.10	7.78	0.16	6.40	0.17	9.19	0.18	9.06	0.21	26.43	0.61
Sm	2.51	0.12	2.61	0.10	2.29	0.07	3.03	0.10	2.93	0.08	5.84	0.09
Eu	0.97	0.04	1.03	0.02	0.92	0.04	1.11	0.03	1.12	0.04	1.82	0.06
Gd	3.28	0.06	3.39	0.10	3.13	0.09	3.71	0.07	3.66	0.06	5.61	0.13
Tb	0.58	0.03	0.59	0.03	0.55	0.02	0.65	0.02	0.63	0.04	0.86	0.03
Dy	4.18	0.13	4.28	0.15	3.93	0.07	4.55	0.09	4.39	0.11	5.45	0.14
Ho	0.89	0.01	0.88	0.04	0.84	0.02	0.97	0.01	0.93	0.03	1.08	0.04
Er	2.50	0.08	2.49	0.03	2.38	0.04	2.70	0.06	2.61	0.06	2.98	0.08
Tm	0.36	0.01	0.35	0.00	0.36	0.01	0.38	0.02	0.35	0.01	0.45	0.01
Yb	2.60	0.11	2.57	0.03	2.41	0.07	2.73	0.02	2.71	0.04	3.02	0.09
Lu	0.35	0.01	0.37	0.02	0.33	0.02	0.38	0.01	0.36	0.02	0.42	0.02
Hf	1.52	0.11	1.61	0.04	1.37	0.02	1.95	0.03	1.83	0.06	3.87	0.11
Ta	0.04	0.01	0.06	0.01	0.03	0.01	0.16	0.01	0.16	0.00	0.70	0.02
Pb	0.50	0.05	0.65	0.02	0.54	0.05	0.67	0.06	0.75	0.06	14.3	0.3
Th	0.04	0.01	0.07	0.01	0.04	0.01	0.20	0.01	0.21	0.02	5.20	0.12
U	0.02	0.00	0.02	0.01	0.01	0.00	0.07	0.01	0.07	0.00	1.88	0.06

in the crust underlying the vent site, although this is not the case for the Kairei vent site, as previously suggested by Gallant & Von Damm (2006).

Fe concentrations in hydrothermal fluids in MOR environment are controlled by phase equilibria for Fe-bearing minerals (e.g., magnetite, hematite, pyrite, pyrrhotite, chlorite) and by the solubility of Fe in the hydrothermal fluids (Ding & Seyfried 1992; Saccocia & Seyfried 1994). Solubility of Fe is, in turn, controlled by temperature, chloride content and pH (Ding & Seyfried 1992). Although Fe/Cl ratios of both Kairei and Edmond fluids are well within the ranges reported for MOR hydrothermal fluids (Gallant & Von Damm 2006), Fe concentrations of Edmond fluids are more than two times higher than those of Kairei fluids, despite the temperatures of end-member fluids being similar: Kairei 369°C, Edmond 381°C. The difference of the Fe concentrations are partly explainable by the somewhat higher Cl concentrations in the Edmond fluid relative to

the Kairei hydrothermal fluids. In addition, Edmond fluids have lower pH values than Kairei fluids. Even a small decrease of pH in hydrothermal fluids could drastically increase Fe concentration (Ding & Seyfried 1992). Therefore, the difference of pH between Kairei and Edmond fluids appears to be responsible for that of Fe concentrations. It should also be noted that supercritical phase separation of hydrothermal fluids drastically increases the Fe/Cl ratio in the brine phase (Seyfried & Ding 1995). This could also play an important role, explaining the high Fe/Cl ratio of the brine-rich Edmond fluids.

In a typical MOR hydrothermal system, concentrations of H_2 are known to be controlled primarily by redox reactions involving Fe-oxides and Fe-sulphides such as hematite-magnetite and pyrite-pyrrhotite-magnetite. These buffer reactions result in less than approximately 1 mmol kg^{-1} H_2 in the hydrothermal fluids at typical hydrothermal conditions of 350–400°C and 500 bar (e.g., Seyfried & Ding 1995; Wetzel & Shock 2000). The Kairei vent field is on a typical basaltic abyssal hill designated as Hakuho knoll. However, H_2 concentrations of the hydrothermal fluids are surprisingly high, up to one order of magnitude higher than typical MOR hydrothermal fluids. To account for the unusually high concentration of H_2, Gallant & Von Damm (2006) proposed a model whereby H_2 was generated by precipitation reactions of metal sulphide minerals, which relies on reactions of (non-sulphide) iron minerals with H_2S in the hydrothermal fluid. However, to generate the observed concentration of H_2 (approximately 8 mmol kg^{-1}) by metal sulphide-precipitation reactions, very high concentrations of Fe (ca. 13–20 mmol kg^{-1}) in the original fluids are required. This appears to be impossible for the Kairei hydrothermal fluids having seawater-like Cl contents of approximately 600 mmol kg^{-1}. Moreover, despite the fact that such metal sulphide precipitation can plausibly occur in typical MOR hydrothermal systems, almost all known basalt-hosted hydrothermal fluids exhibit much lower H_2 concentrations (approximately one order of magnitude lower) than Kairei fluids (e.g. Wetzel & Shock 2000; Charlou *et al.* 2002).

The discovery, reported here, of the presence of serpentinized olivine-rich rocks exposed near the Kairei vent field suggests an alternative mechanism for generating elevated H_2. The serpentinization of olivine-rich ultramafics such as abyssal peridotite is well-known to generate considerably H_2-enriched hydrothermal fluids (e.g. Wetzel & Shock 2000; Allen & Seyfried 2003). This process might supply H_2 to the Kairei fluids as well as in the other H_2-enriched hydrothermal vent fields along Mid Atlantic Ridge (Charlou *et al.* 2002; Douville *et al.* 2002). Although the dunite, troctolite and olivine gabbro from the Uraniwa-Hills are not typical mantle peridotites, it is noteworthy that these rocks contain substantial amounts of olivine, and have great potential for H_2-production. Indeed, the olivine-rich gabbroic rocks were affected pervasively by serpentinization (Morishita *et al.* 2008), directly indicating the generation of abundant H_2 into the Kairei hydrothermal fluids during hydrothermal alteration.

CONCLUDING REMARKS

The heterogeneous structure of the shallow lithosphere seems to have led to large chemical variations in vent fluids. From this perspective, the distinct chemical fluid compositions of two hydrothermal fields, Kairei and Edmond in the Indian Ocean, are attributable to the different rock facies associated with the pathway of discharged hydrothermal vent fluids. The unique geochemical character of the Kairei vent fluid, which had been explained by unusual geochemical reactions beneath the seafloor by Gallant & Von Damm (2006), can also be explained using the occurrence of unique olivine-rich rock facies in the recharge zone of vent fluid. Rocks of this type are not in the group of the mantle-derived ultramafic rocks, but in the group of the deepest part of the mafic crust and reaction zone between upwelling magma and the surrounding residual mantle rocks at the MOHO transition zone. In contrast, the geochemical characteristics of the Edmond vent fluid are fully explained using the reaction within normal mafic crustal materials with a geochemically-enriched trace element nature. The difference in lithology is largely attributable to the tectonic history in each region. In essence, the limited contribution of the unique rock facies to the Kairei vent fluid is related to its heterogeneous structure, reflecting the complex history of seafloor spreading around the triple junction area. The geophysical and morphological observations described herein support the occurrence of the heterogeneous shallow lithosphere around the Kairei hydrothermal field.

The discovery of olivine-rich troctolites at the Uraniwa Hills leads us to propose its important geological role in the oldest ancestral biological community on the ancient Earth. Probably, only minor exposure of ultramafic mantle rocks occurred during the early stages of Earth's history because of frequent and vigorous volcanism driven by mantle convection. However, certain ultramafic volcanic rocks, designated as komatiites, are widely found in Archaean lithological units (>2.5 Ga). Their geochemical character broadly resembles that of the troctolites found in this expedition: hydrothermal fluid associated with komatiites might have fostered hydrogen-favouring progenitors on ancient Earth.

ACKNOWLEDGEMENTS

We would like to thank the officers, crews and technitians of R/V Yokosuka, the pilots of Shinkai6500 Submersible, and related scientists for their help and assisttance

throughout the expedition. We are especially grateful to Prof. Arai and Dr. Ishida of Kanazawa Univ. for their providing us accomodations to measure trace elements of glass samples with LA-ICP-MS. This study used the data and samples acquired during YK05-16 and related cruises of R/V Yokosuka and DSRV Shinkai6500 of JAMSTEC. HK also thank Mr. B. Fast and his colleagues for their English editing for the main part of the manuscript. Constructive comments by two anonymous reviewers and by editor Richard Worden greatly improved this paper. This research was supported by the following grants: Grants-in-Aid for Scientific Research from the Ministry of Education, Culture, Sports, Science and Technology of Japan (MEXT; No. 14253003); JAMSTEC multi-disciplinary research promotion grant entitled 'An interaction of mantle and life through Earth history'. The cruise was conducted as a part of Deep Sea Research Programme funded by MEXT.

REFERENCES

Allen DE, Seyfried WE Jr (2003) Conpositional controls on vent fluids from ultramafic-hosted hydrothermal systems at mid-ocean ridges: An eperimental study at 400°C, 500 bars. *Geochimica et Cosmochimica Acta*, **67**, 1531–42.

Bach W (2007) *Geochemical Diversity of Hydrothermal Systems: Thermodynamic Constraints on Biology*, InterRidge Theoretical Institute:Biogeochemical Interaction at Deep-Sea VentsWoods Hole Sept 10–4 InterRidge, Woods Hole (http://interridge.whoi.edu/files/interridge/Bach_IRTI.pdf).

Beltenev V, Ivanov V, Rozhdestvenskaya I, Cherkashov G, Stepanova T, Shilov V, Pertsev A, Davydov M, Egorov I, Melekestseva I, Narkevsky E, Ignatov V (2007) A new hydrothermal field at 13°30′N on the Mid-Atlantic Ridge. *Interridge Newsletter*, **16**, 9–10.

Berndt ME, Seyfried WE Jr (1993) Calcium and sodium exchange during hydrothermal alteration of calcic plagioclase at 400°C and 400 bars. *Geochimica et Cosmochimica Acta*, **57**, 4445–51.

Berndt ME, Seyfried WE Jr, Janecky DR (1989) Plagioclase and epidote buffering of cation ratios in mid-ocean ridge hydrothermal fluids: Experimental results in and near the supercritical region. *Geochimica et Cosmochimica Acta*, **53**, 2283–300.

Blair CC, D'Hondt S, Spivack AJ, Kingsley RH (2007) Radiolytic hydrogen and microbial respiration in subsurface sediments. *Astrobiology*, **7**, 951–70.

Briais A (1995) Structural analysis of the segmentation of the Central Indian Ridge between 20°30′S and 25°30′S (Rodriguez Triple Junction). *Marine Geophysical Research*, **17**, 431–67.

Charlou JL, Donval JP, Fouquet Y, Jean-Baptiste P, Holm N (2002) Geochemistry of high H_2 and CH_4 vent fluids issuing from ultramafic rocks at the Rainbow hydrothermal field (36°14′N, MAR). *Chemical Geology*, **191**, 345–59.

Ding K, Seyfried WE Jr (1992) Determination of Fe-Cl complexing in the low pressure supercritical region (NaCl fluid): Iron solubility comstraints on pH of subseafloor hydrothermal fluids. *Geochimica et Cosmochimica Acta*, **56**, 3681–92.

Douville E, Charlou JL, Oelkers EH, Bienvenu P, Jove Colon CF, Donval JP, Fouquet Y, Prieur D, Apriou P (2002) The rainbow vent fluids (36°14′N, MAR): the influence of ultramafic rocks and phase separation on trace metal content in Mid-Atlantic Ridge hydrothermal fluids. *Chemical Geology*, **184**, 37–48.

Gallant RM, Von Damm KL. (2006) Geochemical controls on hydrothermal fluids from the Kairei and Edmond Vent Fields, 23°-25°S, Central Indian Ridge. *Geochemistry Geophysics Geosystems*, **7**, Q06018, doi:10.1029/2005GC001067.

Gamo T, Chiba H, Yamanaka T, Okudaira T, Hashimoto J, Tsuchida S, Ishibashi J-i, Kataoka S, Tsunogai U, Okamura K, Sano Y, Shinjo R (2001) Chemical characteristics of newly discovered black smoker fluids and associated hydrothermal plumes at the Rodriguez Triple Junction, Central Indian Ridge. *Earth and Planetary Science Letters*, **193**, 371–9.

Hellebrand E, Snow JE, Hoppe P, Hofmann AW (2002) Garnet-field melting and late-stage refertilization in 'residual' abyssal peridotites from the Central Indian Ridge. *Journal of Petrology*, **43**, 2305–38.

Hessler RR, Kaharl VA (1995) The deep-sea hydrothermal vent community: an overview. In: *Seafloor Hydrothermal Systems* (eds Humphris SE, Zierenberg RA, Mullineaux LS, Thomson RE), *Geophysical Monograph*, **91**, 72–84.

Honsho C, Tamaki K, Fujimoto H (1996) Three-dimensional magnetic and gravity studies of the Rodriguez Triple Junction in the Indian Ocean. *Journal of Geophysical Research*, **101**, 15837–48.

Ishida Y, Morishita T, Arai S, Shirasaka M (2004) Simultaneous in-site multi-element analysis of minerals on thin section using LA-ICP-MS. *The Science Reports of Kanazawa University*, **48**, 31–42.

Kawagucci S, Toki T, Ito M, Oomori T, Ishibashi J, Masuda H, Takai K, Gamo T (2007) Anomalously low D/H ratio of H_2 gas from high temperature hydrothermal fluids in the Mariana Trough. *Geochimica et Cosmochimica Acta*, **71**, A472.

Kelley DS, Karson JA, Früh-Green GL, Yoerger DR, Shank TM, Butterfield DA, Hayes JM, Schrenk MO, Olson EJ, Proskurowski G, Jakuba M, Bradley A, Larson B, Ludwig K, Glickson D, Buckman K, Bradley AS, Brazelton WJ, Roe K, Elend MJ, Delacour A, Bernasconi SM, Lilley MD, Baross JA, Summons RE, Sylva SP (2005) A serpentinite-hosted ecosystem: the lost city hydrothermal field. *Science*, **307**, 1428–34.

Konno U, Tsunogai U, Nakagawa F, Nakaseama M, Ishibashi J, Nunoura T, Nakamura K (2006) Liquid CO_2 venting on seafloor: Yonaguni IV Knoll hydrothermal system, Okinawa trough. *Geophysical Research Letters*, **33**, L16607, doi:10.1029/2006GL026115.

Longerich HP, Jackson SE, Günther D (1996) Laser ablation inductively coupled plasma mass spectrometric transient signal data acquisition and analyte concentration calculation. *Journal of Analytical Atomic Spectrometry*, **11**, 899–904.

Macdonald GA, Katsura T (1964) Chemical composition of Hawaiian lavas. *Journal of Petrology*, **5**, 82–133.

McLaughlin-West EA, Olson EJ, Lilley MD, Resing JA, Lupton JE, Baker ET, Cowen JP (1999) Variations in hydrothermal methane and hydrogen concentrations following the 1998 eruption at axial volcano. *Geophysical Research Letters*, **26**, 3453–6.

Mitchell N, Escartin J, Allerton S (1998) Detatchment faults at Mid-Ocean Ridges garner interest. *EOS Transactions AGU*, **79**, 127.

Morishita T, Ishida Y, Arai S (2005a) Simultaneous determination of multiple trace element compositions in thin (< 30 μm) layers of BCR-2G by 193nm ArF excimer laser ablation-ICP-MS: implications for matrix effect and element fractionation on quantitative analysis. *Geochemical Journal*, *39*, 327–40.

Morishita T, Ishida Y, Arai S, Shirasaka M (2005b) Determination of multiple trace element compositions in thin (< 30 μm) layers of NIST SRM 614 and 616 using laser ablation ICP-MS. *Geostandard Geoanalytical Research*, *29*, 107–22.

Morishita T, Nakamura K, Sawaguchi T, Hara K, Arai S, Kumagai H (2008) Elemental mobilizations during hydrothermal alteration of oceanic lithosphere. *Journal of Geography*, **117**, 220–52.

Nakamura K, Kato Y, Tamaki K, Ishii T (2007) Geochemistry of hydrothermally altered basaltic rocks from the Southwest Indian Ridge near the Rodriguez Triple Junction. *Marine Geology*, **239**, 125–41.

Nozaki Y (2001) Elemental distribution. In: *Encyclopedia of Ocean Sciences Vol.2* (eds Steele JH, Turekian KK, Thorpre SA), pp. 840–5. Academic Press, San Diego.

Pearce NJG, Perkins WT, Westgate JA, Gorton MP, Jackson SE, Neal CR, Chenery SP (1997) A compilation of new and published major and trace element data for NIST SRM 619 and NIST SRM 612 glass reference materials. *Geostandards Newsletter*, **21**, 115–44.

Saccocia PH, Seyfried WE Jr (1994) The solubility of chlorite solid solutions in 3.2 wt% NaCl fluids from 300-400°C, 500 bars. *Geochimica et Cosmochimica Acta*, **58**, 567–85.

Saegusa S, Tsunogai U, Nakagawa F, Kaneko S (2006) Development of a multi-bottle gas-tight fluid sampler WHATS II for Japanese submersibles/ROVs. *Geofluids*, **6**, 234–40.

Seyfried WE Jr, Ding K (1995) Phase equilibria in subseafloor hydrothermal systems: a review of the role of redox, temperature, pH and dissolved Cl on the chemistry of hot spring fluids at mid-ocean ridges. In: *Seafloor Hhydrothermal Systems: Physical, Chemical, Biologic, and Geological Interactions* (eds Humphris SE, Zierenberg RA, Mullineaux LS, Thomson RE), *Geophysical Monograph*, **91**, pp. 248–73. American Geophysical Union, Washington, DC.

Sun S-s, McDonough WF (1989) Chemical and isotopic systematics of oceanic basalts: implications for mantle composition and processes. In: *Magmatism in the Ocean Basins* (eds Saunders AD, Norry MJ), **42**, pp. 313–45. Geological Society of London Spcecial Publication, Blackwell, Oxford.

Takai K, Gamo T, Tsunogai U, Nakayama N, Hirayama H, Nealson KH, Horikoshi K (2004) Geochemical and microbiological evidence for a hydrogen-based, hyperthermophilic subsurface lithoautotrophic microbial ecosystem (HyperSLiME) beneath an active deep-sea hydrothermal field. *Extremophiles*, **8**, 269–82.

Takai K, Nakagawa S, Reysenbach A-L, Hoek J (2006) Microbial ecology of Mid-Ocean Ridges and Back-Arc Basins. In: *Back-Arc Spreading Systems - Geological, Biological, Chemical, and Physical Interactions* (eds Christie DM, Fisher CR, Lee S-M, Givens S) *Geophysical Monograph*, **166**, pp. 185–213. American Geophysical Union, Washington, DC.

Tsunogai U, Toki T, Nakayama N, Gamo T, Kato H, Kaneko S (2003) WHATS: a new multi-bottle gas-tight sampler for seafloor vent fluids. *Chikyukagaku (Geochemistry)*, **37**, 101–9.(in Japanese with English abstract).

Van Dover CL, Humphris SE, Fornari D, Cavanaugh CM, Collier R, Goffredi SK, Hashimoto J, Lilley MD, Reysenbach AL, Shank TM, Von Damm KL, Banta A, Gallant RM, Götz D, Green D, Hall J, Harmer TL, Hurtado LA, Johnson P, McKiness ZP, Meredith C, Olson E, Pan IL, Turnipseed M, Won Y, Young CR III, Vrijenhoek RC (2001) Biogeography and ecological setting of indian ocean hydrothermal vents. *Science*, **294**, 818–23.

Wakabayashi N (2003) *Geophysical Study of the Rodriguez Triple Junction and the Southernmost Part of the Central Indian Ridge.* Master's Thesis, University of Tokyo, Tokyo.

Walter M, Mertens C, Stöber U, Rhein M (2008) Mixing, internal waves, and plume dispersal at the Nibelungen hydrothermal site, southern MAR. *Geophysical Research Abstracts*, **10**, EGU2008-A-11641: OS17/SM20-IM.3P-0614.

Wetzel LR, Shock EL (2000) Distinguishing ultramafic- from basalt-hosted submarine hydrothermal systems by comparing calculated vent fluid compositions. *Journal of Geophysical Research*, **105**, 8319–40.